

Monitoring of water content and water distribution in ischemic hearts

M. Schaefer*, W. Gross, M. Preuss, J. Ackemann, M.M. Gebhard

Department of Experimental Surgery, University of Heidelberg, Im Neuenheimer Feld 365, D-69120 Heidelberg, Germany

Received 3 March 2003; received in revised form 5 June 2003; accepted 1 August 2003

Abstract

We determined water content and water distribution by fitting dielectric spectra of ischemic canine hearts between 5 MHz and 3 GHz with a newly developed model which describes heart cells and subcellular organelles as rotational ellipsoids filled with electrolyte enclosed by an isolating membrane. The fraction of dry material is modelled by spherical particles with a small dielectric permittivity. Free model parameters were water content, cell volume fraction, and the conductivity of the electrolytes. Resulting model parameters were compared to data from tissue desiccation and to conductivity changes produced by protons and lactate ions. We investigated hearts in two states: during ischemia after interruption of blood flow (pure ischemia, PI, $n=5$) and during ischemia after resuscitation with Tyrode's solution (IAR, $n=14$).

The difference between water content determined by tissue desiccation and by dielectric spectroscopy was less than 0.5%. During 360 min of ischemia, water content in IAR decreased from $85 \pm 1.6\%$ to $83 \pm 2.2\%$ and in PI from $80 \pm 0.8\%$ to $78 \pm 1.5\%$. Cellular volume fraction in IAR increased from 0.47 ± 0.045 to 0.63 ± 0.031 and in PI from 0.62 ± 0.014 to 0.73 ± 0.013 , which is consistent with published morphometric data. After 180 min of ischemia, the increase of the cytosolic conductivity was 0.14 ± 0.02 S/m as calculated from the dielectric spectrum and was similar to the conductivity increase which was roughly estimated on the basis of tissue lactate concentration.

In conclusion, dielectric spectroscopy combined with our model analysis facilitates the monitoring of water content and distribution by means of nondestructive surface probes.

© 2003 Elsevier B.V. All rights reserved.

Keywords: Dielectric spectroscopy; Heart; Ischemia; Tissue model; Water content; Water distribution

1. Introduction

The exchange of water between the different body fluid compartments is facilitated by two forces: hydrostatic pressure and osmotic pressure. Constancy of the internal environment is maintained by several body systems. Any perturbation of this balance may cause changes of tissue water content as well as of water distribution, e.g. by shifts of water between extra- and intracellular volume [1]. Such a perturbation could be the result from changes of cell structure caused by tumour growth [2–4], from changes of membrane permeability [5,6], from metabolic tissue diseases [7], from traumatic injury [6], or from ischemia [8,9]. In cardiac muscle tissue, water distribution is also correlated with contractile function [10]. Therefore, monitoring water content and water distribution in tissue may

help to assess its state of health [11]. However, in vivo measurement of water content and water distribution is still a problem. Simple methods like drying and weighing tissue samples to obtain water content [12] or measurement of the distribution of tracers or dye markers [5,13] are invasive and cannot be applied to living tissue. Water content can be determined non-invasively by the nuclear magnetic resonance method [14–16], but this method is expensive and discrimination between intra- and extracellular water is difficult. Water distribution can be estimated from passive electrical impedance measurements [13,17], a method that does not harm the tissue and is easy to apply but requires the precise knowledge of the specific conductivity of each compartment [18]. However, during organ ischemia, anaerobic metabolism causes unknown variations of the conductivity of each electrolytic compartment [19] and changes of membrane properties [20] which reduce the accuracy of water content and water distribution measurements by the impedance technique [18]. To overcome this difficulty, we used the complex dielectric spectrum consisting of the dielectric permittivity ϵ' and the conductivity σ .

* Corresponding author. Tel.: +49-6221-56-1755; fax: +49-6221-56-4208.

E-mail address: michael.schaefer@exchi.uni-heidelberg.de (M. Schaefer).

Dielectric permittivity ϵ' of biological tissue mainly depends on water content and on water distribution between intra- and extracellular volume and is not much affected by variation of the electrolyte's conductivity [21]. The contribution of water molecules to the dielectric properties of biological tissue can be seen beyond several hundreds of MHz; however, it is hidden behind other dielectric polarisation processes like Maxwell–Wagner polarisation of membranes in the biological tissue [22]. A suitable tissue model is required in order to separate the water contribution from other polarisation mechanisms. In Ref. [23], we presented a tissue model which facilitates the analysis of dielectric spectra of heart during ischemia. It considered cell shape and the polarisation of membranes of cells and intracellular structures. Free model parameters were the cellular volume fraction and the conductivity of each electrolytical compartment. Since this model was not sufficient to extract water content, we had to resort to a different mixture formula. To overcome this restriction, we enhanced the model of Ref. [23] in this work by adding structures representing the dry matter of heart tissue.

To test the model, we investigated hearts during ischemia after interruption of blood circulation and hearts during ischemia after resuscitation with Tyrode's solution. The parameters calculated with the dielectric model were compared to inraischemic tissue lactate concentration and to changes of tissue pH caused by anaerobic metabolism [24], to cell edema independently measured by the analysis of histologic slices of heart tissue [25], and to water content determined by drying and weighing tissue samples.

2. Materials and methods

2.1. Experimental procedure

All animals received humane care according to the Guide for the Care and Use of Laboratory Animals (NIH, pub. 86-23, revised 1985). The experiments were performed on canine hearts (Foxhounds) during ischemia at 25 °C. Two experimental groups were investigated: ischemic hearts after resuscitation with Tyrode's solution (IAR, $n = 14$) and hearts during pure ischemia (PI, $n = 5$). The group of resuscitated hearts was part of other experiments with the purpose to investigate the effect of ischemic damage on postischemic function after resuscitation. Similar experiments are described in Ref. [26]. These hearts were preischemically perfused with HTK solution (Custodiol®, Köhler Chemie, Alsbach-Hähnlein, Germany), then excised and stored at 5 °C during a first ischemia period. After 480 min of ischemia, they were reperused with Tyrode's solution at 37 °C for 90 min. We investigated these hearts during the second period of ischemia at 25 °C following reperfusion. Pure ischemic hearts were excised directly after interruption of blood circulation, cooled in 5 °C Ringer's solution (Braun Melsungen, Melsungen Germany) for about 5 min

and stored at 25 °C during ischemia. Investigations started about 10 min after the onset of ischemia.

2.2. The dielectric spectrum of heart and water content

A sample of the right ventricular myocardium (2.5×2.5 cm) was dissected, weighed and positioned on the aperture of a coaxial line which ended in the flat metal plate of the sample chamber. The sample chamber was kept at 25 °C and had a plastic cover in order to avoid desiccation of the tissue. The complex reflection coefficient of the interface between coaxial line and tissue was measured from 5 MHz to 3 GHz every 10 min during ischemia by using a network analyzer HP 8753C in combination with an S-parameter test set HP 86046 A (Hewlett Packard, Palo Alto, USA). The complex dielectric permittivity of the heart tissue was calculated from the reflection coefficient measured after system calibration of the open-ended coaxial line with three standards: air, short circuit, and an aqueous solution of 0.05 mol/l NaCl [23]. At the end of each experiment, the heart sample was weighed, its volume determined, then dried for 48 h at 100 °C, and weighed again. Water content was calculated from the wet to dry ratio and the density ρ_{dm} of the dry matter was determined by Eq. (1).

$$\rho_{dm} = \frac{m_{dm}}{V_s - \frac{m_w}{\rho_w}} \quad (1)$$

with V_s = volume of the tissue sample, m_{dm} = mass of the dry matter, m_w = mass of tissue water, and water density $\rho_w = 1$ g/cm³.

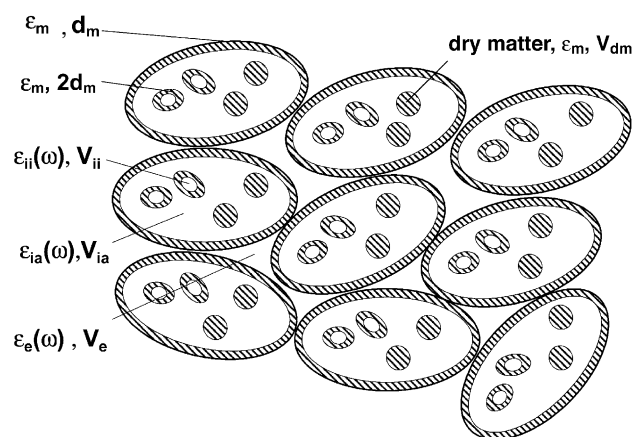


Fig. 1. The simplified model of heart tissue as previously described in Ref. [23] was enhanced by introducing intracellular spherical particles with volume V_{dm} and dielectric permittivity $\epsilon_m = 5$ representing the dry matter. The model consists of three compartments filled with electrolytic solutions: the extracellular volume V_e ($\epsilon_e(\omega)$), intracellular volume V_{ia} ($\epsilon_{ia}(\omega)$), and the internal volume of subcellular structures like mitochondria V_{ii} ($\epsilon_{ii}(\omega)$). The three compartments are separated from each other by membranes with thickness d_m and dielectric permittivity $\epsilon_m = 5$. The dielectric properties $\epsilon_k(\omega)$, $k = e, ia, ii, m$, are calculated by using the Cole–Cole spectral function [27], $\omega = 2\pi f$, f = frequency.

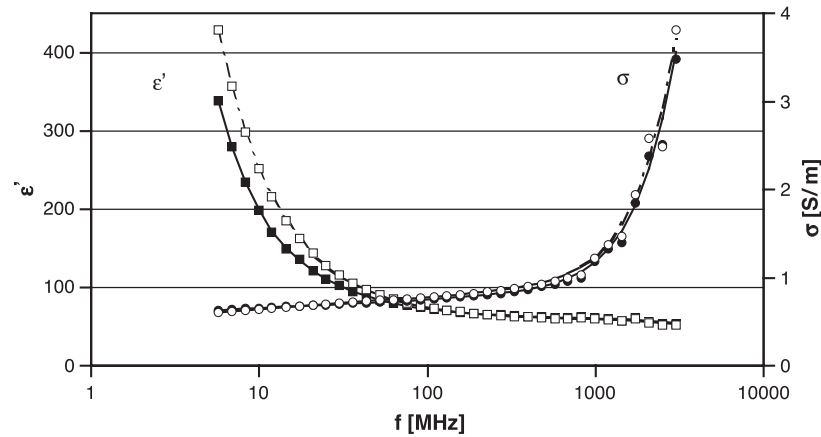


Fig. 2. Representative spectra of dielectric permittivity $\epsilon'(f)$ and conductivity $\sigma(f)$ of heart tissue at 25 °C measured at 30 min (filled symbols) and 300 min (open symbols) after the onset of pure ischemia (PI). The lines were calculated by the electrical heart model (solid line at 30 min and broken line at 300 min). Mean square was 0.67 at 30 min and 0.86 at 300 min.

2.3. The dielectric heart model and data analysis

The tissue model shown in Fig. 1 uses ellipsoids enclosed by isolating membranes to describe the electrical properties of myocardial cells or of cell organelles like mitochondria or nuclei. It is based on a previously described model [23] and was enhanced by introducing intracellular spherical particles consisting of nonpolar dielectric matter which allow for the effect of the dry matter on the dielectric properties of myocardial tissue. Intracellular structures are embedded in the cytosolic electrolyte and the concentration is given by the volume fraction

$$v_{ii} = \frac{V_{ii}}{V_e + V_{ia} + V_{ii} + V_{dm}} \quad (2)$$

with the extracellular volume V_e , the intracellular volume V_{ia} , the internal volume of subcellular structures like mito-

chondria V_{ii} , and the volume V_{dm} of intracellular spherical particles (cf. Fig. 1). The concentration of the cellular ellipsoids in the extracellular space is given by the cellular volume fraction.

$$v_i = \frac{V_{ia} + V_{ii} + V_{dm}}{V_e + V_{ia} + V_{ii} + V_{dm}} \quad (3)$$

The dielectric permittivity of the model was calculated by using a mixture formula which is suitable for high volume fractions of the dissolved ellipsoidal component. The mixture formula and a general expression of the dielectric permittivity associated to this model was described in detail in Ref. [23]. The calculations were performed in four steps: (1) The determination of the effective dielectric permittivity of the membrane-enclosed ellipsoids symbolising the cell organelles. (2) The effective

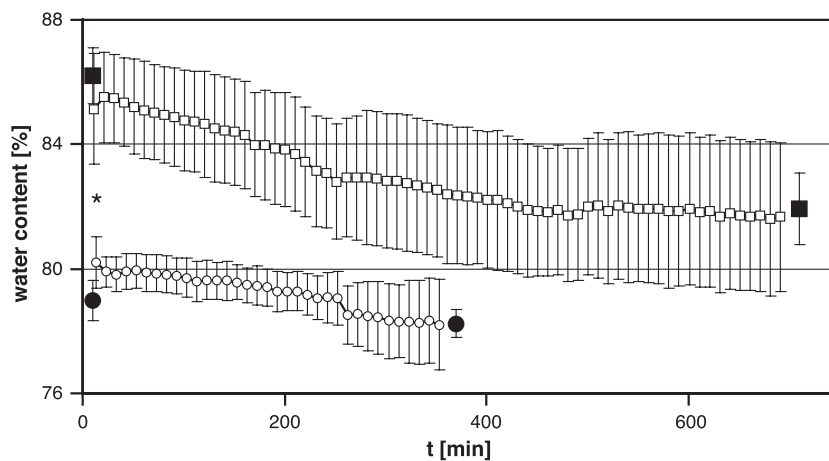


Fig. 3. Water content of pure ischemic hearts (PI, circle symbols, $n=5$) in comparison to water content of hearts during ischemia after resuscitation with Tyrode's solution (IAR, square symbols, $n=14$). Two methods were used for measurements: drying and weighing of heart samples (filled symbols) and analysis of the complex dielectric permittivity spectrum measured between 5 MHz and 3 GHz using the heart model (open symbols). Temperature during ischemia was 25 °C (mean \pm S.D.; *PI vs. IAR tested at 13 min, $p < 0.01$).

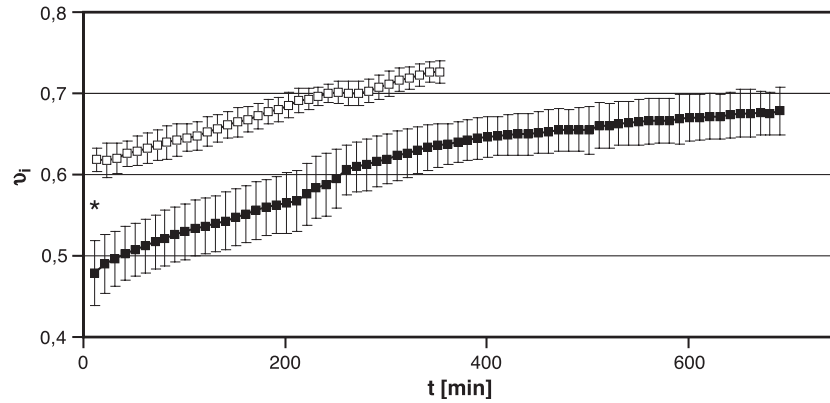


Fig. 4. Intracellular volume fraction v_i for hearts during pure ischemia (PI, open symbols, $n=5$) in comparison to hearts during ischemia after resuscitation with Tyrode's solution (IAR, filled symbols, $n=14$). Data were calculated by analysing the complex dielectric permittivity spectrum measured between 5 MHz and 3 GHz with the heart model. Temperature during ischemia was 25 °C (mean \pm S.D.; *PI vs. IAR tested at 13 min, $p<0.01$).

dielectric permittivity of the cytosol with its embedded particles. (3) The effective dielectric permittivity of the membrane-enclosed ellipsoids representing the tissue cells. (4) The effective dielectric permittivity of the extracellular electrolyte with its embedded cellular ellipsoids. In each step, the electrical properties of all electrolytic model compartments, indexed in Fig. 1 by $k=e$, ia and ii , were calculated with the Cole–Cole spectral function [27]. The following model parameters were kept constant: the static dielectric permittivity $\epsilon'_k(0)=78$, the dielectric relaxation time $\tau_e=9$ ps in the extracellular space, $\tau_{ia}=\tau_{ii}=25$ ps in the intracellular space, and the dielectric permittivity $\epsilon'_k(\infty)=5$ at very high frequencies. Five parameters were subject to a fit algorithm: the volume fraction v_{dm} of the dry matter, the volume fraction v_i of the cells, and the three conductivity parameters σ_k , $k=e$, ia and ii . The dielectric spectrum of the model was fitted to the intraischemically measured data of heart tissue by using a nonlinear least squares fitting algorithm [23].

2.4. Myocardial lactate concentration, tissue pH and their correlation with conductivity

The left ventricles of the pure ischemic hearts were incubated at 25 °C in a beaker filled with Ringer's solution. Tissue biopsies taken during ischemia were homogenised in cold 3.5% perchloric acid and protein was removed by centrifugation. The acid extracts were neutralised, filtered and lactate was assayed enzymatically based on photometric absorbance measurements [26]. The mobility of lactate molecules was determined in an aqueous solution of 0.05 mol/l Na-lactate by measuring the conductivity σ and calculating the mobility μ by Eq. (4)

$$\mu = \frac{\sigma - ne\mu_{Na}}{ne} \quad (4)$$

with the number of ions n , the elementary charge $e=1.6 \times 10^{-19}$ C, and the mobility of Na ions $\mu_{Na}=4.6 \times 10^{-8}$ m²/Vs. During ischemia, we calculated

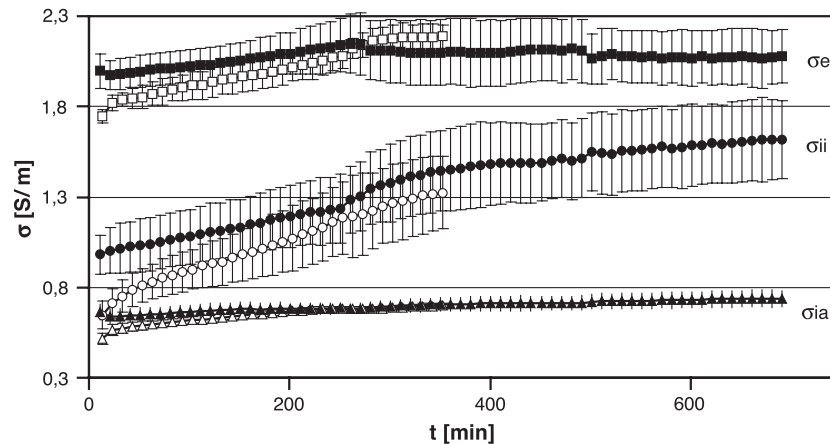


Fig. 5. Conductivity of extracellular electrolyte σ_e , cytosol σ_{ia} and inner electrolyte of cell organelles σ_{ii} for hearts during pure ischemia (PI, open symbols, $n=5$) in comparison to hearts during ischemia after resuscitation with Tyrode's solution (IAR, filled symbols, $n=14$). Data were calculated by analysing the complex dielectric permittivity spectrum measured between 5 MHz and 3 GHz with the heart model. Temperature during ischemia was 25 °C (mean \pm S.D.).

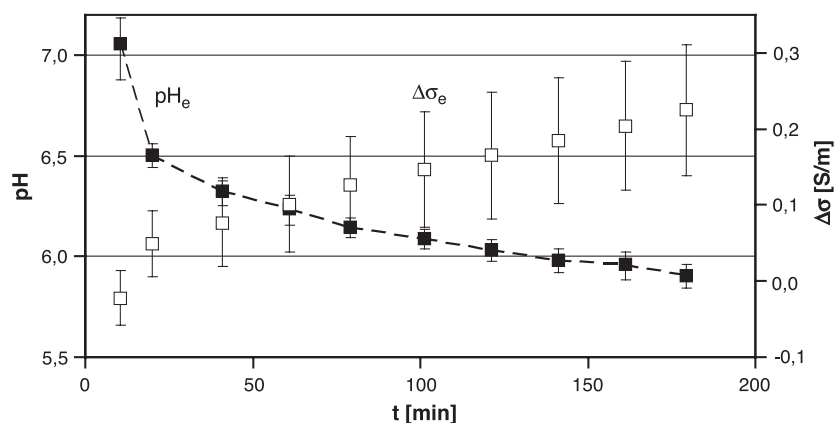


Fig. 6. Extracellular pH_e (filled symbols) measured in hearts during pure ischemia (PI, $n=5$) in comparison to changes of extracellular conductivity $\Delta\sigma_e$ (open symbols) calculated from the complex dielectric permittivity spectrum measured between 5 MHz and 3 GHz using the heart model. Temperature during ischemia was 25 °C (mean \pm S.D.).

the increase of conductivity caused by the measured lactate concentration with Eq. (5)

$$\Delta\sigma_{\text{lactate}} = ne\mu \quad (5)$$

Septum specimens (3×3 cm) were incubated in glass chambers at 25 °C. No bath medium was added but chambers were sealed to avoid desiccation. Tissue pH of these specimens was continuously measured by using micro-pH electrodes with a tip diameter of 1.7 mm (WPI Laboratory Equipment, Hertfordshire, UK). In order to estimate the effect of tissue pH on extracellular electrolyte conductivity, we measured the conductivity of blood plasma subject to pH variations between 5.5 and 7.4.

2.5. Statistics

The measured results are quoted as mean \pm standard deviation (S.D.). Statistical differences between data sets

were calculated by Wilcoxon rank sum test. The null hypothesis was rejected when $p \leq 0.05$.

3. Results

During ischemia, the frequency course of dielectric permittivity ϵ' and of conductivity σ of heart tissue changes in a characteristic way. Fig. 2 shows a representative example from the PI group. With increasing frequency the dielectric permittivity ϵ' decreased while conductivity σ increased. Between 30 min and 300 min, ϵ' increased at frequencies below 100 MHz and showed a small decrease between 200 MHz and 3 GHz. Simultaneously, σ decreased slightly below 20 MHz and increased beyond. When fitting these changes of the spectra during ischemia with the heart model, the parameters varied as demonstrated in Figs. 3–5.

To compare the water content, $1 - v_{\text{dm}}$, as determined by dielectric data analysis, with the results of tissue desiccation,

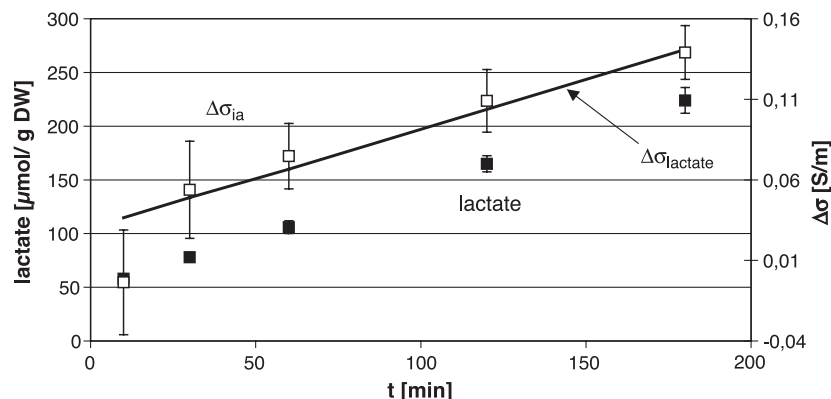


Fig. 7. Lactate concentration (filled symbols) measured in hearts during pure ischemia (PI, $n=5$) and its associated changes of conductivity $\Delta\sigma_{\text{lactate}}$ as calculated with Eq. (5) (solid line) compared to changes of intracellular conductivity $\Delta\sigma_{\text{ia}}$ (open symbols) as calculated from the complex dielectric permittivity spectrum measured between 5 MHz and 3 GHz using the heart model. Temperature during ischemia was 25 °C (DW = dry weight; mean \pm S.D.).

it was necessary to convert v_{dm} into a weight ratio using the density $\rho_{\text{dm}} = 1.4 \pm 0.2 \text{ g/cm}^3$. At the end of measurements, the values calculated by the two methods matched very well but at the start of measurements the dielectrically determined water content was higher in PI (n.s.) but smaller in IAR (n.s.) as compared to water content gained by tissue desiccation (Fig. 3). Water content in IAR decreased from about $85 \pm 1.6\%$ to $82 \pm 2.7\%$ after 700 min while water content in PI started significantly lower at $80 \pm 0.8\%$ ($p < 0.01$) and decreased to $78 \pm 1.5\%$ after 360 min. A reversed relation was obtained for the cellular volume fraction v_i (Fig. 4). This parameter increased in both groups during ischemia but v_i in PI was higher at each time point: in PI, v_i varied from about 0.62 ± 0.014 to 0.73 ± 0.013 after 360 min while v_i in IAR started significantly lower at 0.47 ± 0.045 ($p < 0.01$) and increased to 0.68 ± 0.031 after 700 min. Fitting the dielectric heart data during ischemia required also the variation of the three conductivity parameters σ_e , σ_{ia} , and σ_{ii} of the model (cf. Fig. 1). All three parameters increased and beyond 50 min we found no significant difference between PI and IAR for each parameter (Fig. 5, tested at 100 and 300 min), but up to about 50 min all three conductivity parameters showed lower values in PI.

In PI, extracellular pH_e decreased from about 7 to 5.8 and σ_e increased by approximately 0.25 S/m (Fig. 6). This increase of σ_e is greater than 0.01 S/m, as found in independent measurements on blood plasma when pH varied from 7.0 to 5.8. As shown in Fig. 7, lactate concentration increased during ischemia and we estimated its effect on electrolyte conductivity. From Eq. (4) we obtained the mobility of lactate ions $\mu = 2.61 \times 10^{-8} \text{ m}^2/\text{Vs}$ and used Eq. (5) to calculate the change of conductivity. With the assumption that the lactate ions were distributed homogeneously in all electrolytic compartments of the heart model, the increase of conductivity $\Delta\sigma_{\text{lactate}}$ produced by lactate ions in Fig. 7 was similar to the increase of the conductivity $\Delta\sigma_{\text{ia}}$ calculated by the model.

4. Discussion

Within the scope of the model of Fig. 1, we obtained a reasonably good fit to the measured data as shown in Fig. 2. To estimate the quality of the heart model, we compared the free parameters with results from independent measurements.

4.1. Water content

Water content of heart tissue decreased as a result of the measurement setup because water trickled out through the cutting edges of the samples. Fluid accumulated during ischemia on the floor of the measuring chamber especially with hearts in group IAR which were resuscitated with Tyrode's solution. The discrepancy between results of

individual experiments from drying and weighing and the water content calculated from the dielectric spectrum was less than 0.5% at the end of ischemic measurements (cf. Fig. 3). Differences at the beginning of measurements were due to temperature which was about 10 °C in PI but about 35 °C in IAR. High temperature causes a decrease of the effective dipole moment of water molecules by an increase of Brownian motion: the dielectric permittivity of water is about 84 at 10 °C and 75 at 35 °C [28]. Our model does not allow for this temperature effect on the dielectric permittivity which explains the discrepancy at the beginning of the measurements.

4.2. Cellular volume fraction

The model parameter v_i (cellular volume fraction) was confirmed by independent histologic measurements: Schmiedl et al. [25] investigated volume shifts between intra- and extracellular space of pure ischemic canine hearts by using morphometric techniques. They found that at the onset of pure ischemia 16% of the investigated tissue area was occupied by interstitial space and about 22% by tissue clefts. Consequentially, intracellular volume was about 62%. This result equals the intracellular volume fraction v_i (13 min) = 0.62 ± 0.014 determined with our model in pure ischemic hearts 13 min after the onset of ischemia. During ischemia, the volume fraction v_i increased indicating the development of a cellular edema (Fig. 4). Again, this finding is consistent with the results found by tissue morphometry [25]. For example, at 180 min an intracellular volume of about 68% was measured morphometrically which equals our result, v_i (180 min) = 0.68 ± 0.015 .

Cellular volume fraction of resuscitated hearts in IAR started with significantly smaller values (Fig. 4) and tissue water content was significantly higher (Fig. 3) when compared to hearts in PI. During ischemia, however, a large fraction of the water from the extracellular space drained through the cutting edges of the samples in IAR and cellular volume fraction approached to values found in PI. From these results, we conclude that water was pressed into the extracellular volume during perfusion with the Tyrode's solution. However, we cannot decide if this was a result of using a saline solution instead of blood for heart reperfusion or whether it indicated organ damage, e.g. caused by degradation of endothelium during ischemia [29]. This problem will be the objective of further investigations.

4.3. Conductivity parameters

Due to the different starting temperatures in both groups, we obtained initially lower values for the three conductivity parameters of PI (cf. Fig. 5). After temperature equilibration, each parameter increased to a level found for these parameters in IAR. Such an intranscendent increase of conductivity could be expected as a result of anaerobic metabolism

during ischemia [24], which accumulates free charge carriers like protons and lactate molecules.

Our measurements on blood plasma showed that pH barely effects conductivity. Therefore, the decrease of extracellular pH during ischemia in group PI is not a sufficient cause for the increase of extracellular conductivity σ_e (cf. Fig. 6). In contrast, the increase of intracellular conductivity σ_{ia} was similar to $\Delta\sigma_{lactate}$, as estimated by means of Eq. (5) and the inraischemic concentration of lactate ions (cf. Fig. 7), but we are reluctant to see this as the only possible explanation. So far, we considered only the simplified heart model, proton concentration, and concentration of lactate ions. We neglected many other inraischemic processes, e.g. redistribution of K^+ , Na^+ or Ca^+ between cell compartments [30], swelling of mitochondria [31], or perturbations of active and passive membrane properties [32,33]. To our knowledge, there are no published measurements of the specific conductivity σ_e , σ_{ia} and σ_{ii} during ischemia which could be used to check the model results. Inraischemic lactate accumulation might explain the time course of σ_{ia} . In spite of all simplifications, water content and water distribution as calculated by the model matched very well to results of independent measurements.

4.4. Model limitations

Modelling of heart tissue requires many model parameters to describe the dielectric polarisation due to molecular dipole moments, cell membranes and membranes of sub-cellular structures, and additional parameters to allow for the geometry, concentration and distribution of tissue components. In order to minimise the number of model parameters, we made the following basic assumptions: The extracellular and intracellular space as well as the inner space of the subcellular compartments contain water and ions, and the compartments are separated by membranes consisting of nonpolar material. Spheres of the same nonpolar material dissolved in the water of the intracellular compartment describe the dry component of the tissue. The model neglects dielectric polarisation contributions due to amino acids, partial rotation of charged side-groups of and the relaxation of bound water [34], which are small in comparison with the polarisation contribution of membranes. We approximated the cylindrical shape of the heart cells by ellipsoids in order to simplify calculation of the effective dielectric permittivity [23]. As far as possible, we applied values from literature for the dielectric and structural model parameters. However, we found different values for some parameters, e.g. membrane thickness d_m varies between 10×10^{-10} and 100×10^{-10} m, which has a large influence on the calculated parameters [23]. We used $d_m = 55 \times 10^{-10}$ m which is compatible with the commonly accepted value of about $1 \mu\text{F}/\text{cm}^2$ for the membrane capacitance [34].

The resistance $1000\text{--}2000 \Omega \text{ cm}^2$ [35] of an intact resting membrane with thickness 55×10^{-10} m yields a conductivity of $2 \times 10^{-8} \text{ S/m}$. We did not find data of the

inraischemic time course of membrane resistance in cardiac tissue although it is well known that, for example, the relative potassium ion permeability increases during acute ischemia [36]. In order to estimate the influence of the inraischemic variation of the membrane conductivity on the results of the calculated free model parameters, we decreased the membrane conductivity stepwise from 10^{-10} to 10^{-5} S/m , finding a variation of all free parameters of less than 1%. The higher membrane conductivity was assessed by assuming open ion channels for Na^+ , K^+ , Ca^+ and Cl^- . In the worst case, the membrane conductivity would increase to 10^{-5} S/m using a membrane conductivity of $25 \text{ mS}/\text{cm}^2$ (conductivity of Na^+ during action potential) for each ion. These investigations show that the model is robust under variation of membrane conductivity at frequencies beyond 5 MHz.

5. Conclusion

Water content and its distribution between extra- and intracellular volume differed between pure ischemic hearts and hearts during ischemia after resuscitation. Using dielectric spectroscopy in combination with the presented heart model, we could detect these differences and monitor both parameters during ischemia.

References

- [1] U. Kreimeier, Pathophysiology of fluid imbalance, *Crit. Care* 4 (2000) 3–7.
- [2] H. Takahashi, H. Hamada, A. Teramoto, Usefulness of niravoline, an arginine vasopressin inhibitor, on tumour-origin brain oedema, *Acta Neurochir., Suppl.* 76 (2000) 323–327.
- [3] J. Jossinet, M. Schmitt, A review of parameters for the bioelectrical characterization of breast tissue, *Ann. N.Y. Acad. Sci.* 873 (1999) 30–41.
- [4] B. Blad, B. Baldetorp, Impedance spectra of tumour tissue in comparison with normal tissue; a possible clinical application for electrical impedance tomography, *Physiol. Meas.* 17 (1996) 105–115.
- [5] G.E. Plantke, M. Chakir, S. Lehoux, M. Lortie, Disorders of body fluid balance: a new look into the mechanisms of disease, *Can. J. Cardiol.* 11 (1995) 788–802.
- [6] J. Badaut, F. Lasbennes, P.J. Magistretti, L. Regli, Aquaporins in brain: distribution, physiology, and pathophysiology, *J. Cereb. Blood Flow Metab.* 22 (2002) 367–378.
- [7] K. Bendjelid, E. Canet, Y. Gasche, X. Andre-Fouet, D. Revel, M. Janier, Slaughterhouse blood as a perfusate for studying myocardial function under ischemic conditions, *Braz. J. Med. Biol. Res.* 31 (2003) 39–44.
- [8] A.B. Ericsson, S. Takeshima, J. Vaage, Simultaneous antegrade and retrograde delivery of continuous warm blood cardioplegia after global ischemia, *Thorac. Cardiovasc. Surg.* 115 (1998) 716–722.
- [9] K. Sumimoto, T. Matsura, J.I. Oku, Y. Fukuda, K. Yamada, K. Dohi, Protective effect of UW solution on postischemic injury in rat liver: suppression of reduction in hepatic antioxidants during reperfusion, *Transplantation* 62 (1996) 1391–1398.
- [10] E.G. Butchart, W.G. Austen, M.T. McEnany, Influence of contractility on myocardial water distribution during cardiopulmonary bypass, *Thorac. Cardiovasc. Surg.* 82 (1981) 38–44.

- [11] A.E. Cerussi, D. Jakubowski, N. Shah, F. Bevilacqua, R. Lanning, A.J. Berger, D. Hsiang, J. Butler, R.F. Holcombe, B.J. Tromberg, Spectroscopy enhances the information content of optical mammography, *J. Biomed. Opt.* 7 (2002) 60–71.
- [12] R.F. Reinoso, B.A. Telfer, M. Rowland, Tissue water content in rats measured by desiccation, *J. Pharmacol. Toxicol. Methods* 38 (1997) 87–92.
- [13] H.J. Zdolsek, B. Lisander, A.W. Jones, F. Sjöberg, Albumin supplementation during the first week after a burn does not mobilise tissue oedema in humans, *Intensive Care Med.* 27 (2001) 844–852.
- [14] D. Pouliquen, F. Foussard, G. Tanguy, J. Roux, Y. Malthiery, Total and structured water in cancer: an NMR experimental study of serum and tissues in DMBA-induced OF1 mice, *Cell. Mol. Biol.* 47 (2001) 947–957.
- [15] P.P. Fatouros, A. Marmarou, Use of magnetic resonance imaging for in vivo measurements of water content in human brain: method and normal values, *J. Neurosurg.* 90 (1999) 109–115.
- [16] A.G. Cutillo, A.H. Morris, D.C. Ailion, T.A. Case, C.H. Durney, K. Ganesan, F. Watanabe, M. Akhtari, Assessment of lung water distribution by nuclear magnetic resonance. A new method for quantifying and monitoring experimental lung injury, *Am. Rev. Respir. Dis.* 137 (1988) 1371–1378.
- [17] E. Gersing, Monitoring temperature-induced changes in tissue during hypothermia by impedance methods, *Ann. N.Y. Acad. Sci.* 873 (1999) 13–20.
- [18] B.J. Thomas, B.H. Cornish, L.C. Ward, A. Jacobs, Bioimpedance: is it a predictor of true water volume? *Ann. N.Y. Acad. Sci.* 873 (1999) 89–93.
- [19] E. Gersing, Impedance spectroscopy on living tissues for determination of the organ state, *Bioelectrochem. Bioenerg.* 45 (1998) 145–149.
- [20] E. Carmeliet, Cardiac ionic currents and acute ischemia: from channels to arrhythmias, *Physiol. Rev.* 79 (1999) 917–1017.
- [21] G.G. Kramer, E.R. Cardoso, E. Shweddyk, Dielectric measurement of cerebral water content using a network analyzer, *Neurol. Res.* 14 (1992) 255–258.
- [22] K.R. Foster, H.P. Schwan, Dielectric properties of tissues and biological materials: a critical review, *Crit. Rev. Biomed. Eng.* 17 (1989) 25–104.
- [23] M. Schaefer, W. Gross, J. Ackemann, M.M. Gebhard, The complex dielectric spectrum of heart tissue during ischemia, *Bioelectrochemistry* 58 (2002) 171–180.
- [24] M.M. Gebhard, H.J. Bretschneider, P.A. Schnabel, Cardioplegic principles and problems, in: N. Sperelakis (Ed.), *Physiology and Pathophysiology of the Heart*, Kluwer Academic Publishing, Boston, 1989, pp. 655–669.
- [25] A. Schmiedl, P.A. Schnabel, G. Haasis, G. Mall, M.M. Gebhard, J. Richter, H.J. Bretschneider, Influence of pretreatment on interstitial and intracellular space of canine left-ventricular myocardium, *Acta Anat. (Basel)* 138 (1990) 175–181.
- [26] J. Ackemann, W. Gross, M. Mory, M. Schaefer, M.M. Gebhard, Celsior versus Custodiol: early postischemic recovery after cardioplegia and ischemia at 5 °C, *Ann. Thorac. Surg.* 74 (2002) 522–529.
- [27] C.J.F. Böttcher, P. Bordewijk, *Theory of Electric Polarisation*, Elsevier, Amsterdam, 1978.
- [28] U. Kaatz, V. Uhlendorf, Dielectric properties of water at microwave frequencies, *Z. Phys. Chem.* 126 (1981) 152–165.
- [29] A. Schmiedl, J. Richter, P.A. Schnabel, Different preservation of myocardial capillary endothelial cells and cardiomyocytes during and after cardioplegic ischemia (25 degrees C) of canine hearts, *Pathol. Res. Pract.* 198 (2002) 281–290.
- [30] Y. Wang, A. Sostman, R. Roman, S. Stribling, S. Vigna, Y. Hannun, J. Raymond, J.G. Fitz, Metabolic stress opens K⁺ channels in hepatoma cells through a Ca²⁺- and protein kinase alpha-dependent mechanism, *J. Biol. Chem.* 273 (1996) 18107–18113.
- [31] V.A. Saks, T. Tiivel, L. Kay, V. Novel-Chate, Z. Daneshrad, A. Rossi, E. Fontaine, C. Keriell, X. Leverve, R. Ventura-Clapier, K. Anflous, J.L. Samuel, L. Rappaport, On the regulation of cellular energetics in health and disease, *Mol. Cell. Biochem.* 160–161 (1996) 195–208.
- [32] W.E. Cascio, T.A. Johnson, L.S. Gettes, Electrophysiologic changes in ischemic ventricular myocardium: I. Influence of ionic, metabolic, and energetic changes, *J. Cardiovasc. Electrophysiol.* 6 (1995) 1039–1062.
- [33] A. Schmiedl, F. Bach, H. Fehrenbach, P.A. Schnabel, J. Richter, Cellular distribution patterns of lanthanum and morphometry of rat hearts exposed to different degrees of ischemic stress, *Anat. Rec.* 243 (1995) 496–508.
- [34] B. Rigaud, J.-P. Morucci, N. Chauveau, Bioelectrical impedance techniques in medicine, *Crit. Rev. Biomed. Eng.* 24 (1996) 257–351.
- [35] N. Sperelakis, Basis of the cardiac resting potential, in: N. Sperelakis (Ed.), *Physiology and Pathophysiology of the Heart*, Kluwer Academic Publishing, Boston, 1995, pp. 55–76.
- [36] E. Patterson, B.J. Scherlag, R. Lazzara, Cellular electrophysiology and ischemia, in: N. Sperelakis (Ed.), *Physiology and Pathophysiology of the Heart*, Kluwer Academic Publishing, Boston, 1995, pp. 547–563.